Modulated Amplitude Waves and the Transition from Phase to Defect Chaos

Lutz Brusch[1], Martín G. Zimmermann[2,*], Martin van Hecke[1,3], Markus Bär[1], and Alessandro Torcini[4]
[1] *Max-Planck-Institut für Physik komplexer Systeme, Nöthnitzer Straße 38, D-01187 Dresden, Germany*
[2] *Instituto Mediterraneo de Estudios Avanzados, IMEDEA (CSIC-UIB), E-07071 Palma de Mallorca, Spain*
[3] *Center for Chaos and Turbulence Studies, The Niels Bohr Institute, Blegdamsvej 17, 2100 Copenhagen, Denmark*
[4] *Istituto Nazionale di Fisica della Materia, Unità di Firenze, Largo Enrico Fermi 2, I-50125 Firenze, Italy*
(February 4, 2008)

The mechanism for transitions from phase to defect chaos in the one-dimensional complex Ginzburg-Landau equation (CGLE) is presented. We introduce and describe periodic coherent structures of the CGLE, called Modulated Amplitude Waves (MAWs). MAWs of various period P occur naturally in phase chaotic states. A bifurcation study of the MAWs reveals that for sufficiently large period, pairs of MAWs cease to exist via a saddle-node bifurcation. For periods beyond this bifurcation, incoherent near-MAW structures occur which evolve toward defects. This leads to our main result: the transition from phase to defect chaos takes place when the periods of MAWs in phase chaos are driven beyond their saddle-node bifurcation.

PACS numbers: 47.52.+j, 03.40.Kf, 05.45.+b, 47.54.+r

Spatially extended systems can exhibit, when driven away from equilibrium, irregular behavior in space and time: this phenomenon is commonly referred to as *spatio-temporal* chaos [1]. The one-dimensional complex Ginzburg-Landau equation (CGLE):

$$\partial_t A = A + (1 + ic_1)\partial_x^2 A - (1 - ic_3)|A|^2 A \ , \qquad (1)$$

describes pattern formation near a Hopf bifurcation and has become a popular model to study spatiotemporal chaos [1–13]. As a function of c_1 and c_3, the CGLE exhibits two qualitatively different spatiotemporal chaotic states known as phase chaos (when A is bounded away from zero) and defect chaos (when the phase of A displays singularities where $A=0$). The transition from phase to defect chaos can either be hysteretic or continuous; in the former case, it is referred to as L_3, in the latter as L_1 (Fig. 1). Despite intensive studies [5–13], the phenomenology of the CGLE and in particular its "phase"-diagram [5,7] are far from being understood. Moreover, it is under dispute whether the L_1 transition is sharp, and whether a pure phase-chaotic (*i.e.* defect-free) state can exist in the thermodynamic limit [9].

It is the purpose of this paper to elucidate these issues by presenting the mechanism which creates defects in transient phase chaotic states. Our analysis consists of four parts: *(i)* We describe a family of Modulated Amplitude Waves (MAWs), *i.e.*, pulse-like coherent structures with a characteristic spatial period P. *(ii)* A bifurcation analysis of these MAWs reveals that their range of existence is limited by a saddle-node (SN) bifurcation. For all c_1, c_3 within a certain range, we define P_{SN} as the period of the MAW for which this bifurcation occurs. *(iii)* We show that for $P > P_{SN}$, *i.e.*, beyond the SN bifurcation, near-MAW structures display a nonlinear evolution to defects. It is found that, in phase chaos, near-MAWs with various P's are created and annihilated perpetually.

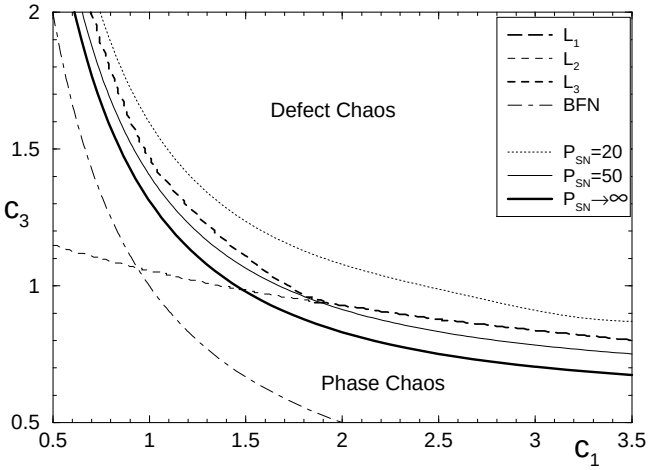

FIG. 1. Phase diagram of the CGLE showing the BFN, L_1, L_2 and L_3 transitions (after [7]). Between the L_2 and L_3 curves, there is the hysteretic regime where either phase or defect chaos can occur; in the latter case, defects persist up to the L_2 transition. Notice how the L_1 and L_3 transitions to defect chaos lie above our lower ($P \to \infty$) bounds. Also shown are the SN locations for $P = 20, 50$.

The transition to defect chaos takes place when near-MAWs with $P > P_{SN}$ occur in a phase chaotic state. *(iv)* Finally, instabilities to splitting of *resp.* interaction between MAWs are identified as the relevant processes which locally decrease *resp.* increase P in phase chaos. We will argue that the SN curve for $P \to \infty$ is a lower bound (see Fig. 1) for the transition from phase chaos to defect chaos.

From a general viewpoint, our analysis shows that there is no collective behavior that drives the transition. Instead, strictly local fluctuations drive local structures beyond their SN bifurcation and create defects.

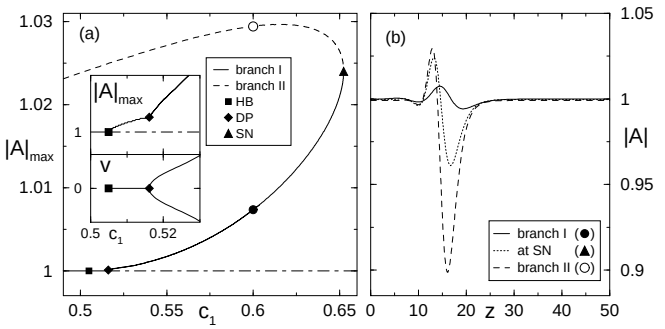

FIG. 2. (a) Example of the bifurcation diagram of MAWs for $c_3 = 2.0, P = 50$ (see text). The inset illustrates the drift pitchfork bifurcation ($v = 0$ branch not shown beyond bifurcation). (b) MAW profiles at lower (full circle) and upper (open circle) branch, and at the SN (triangle).

(i) MAWs as coherent structures - By coherent structures we mean uniformly propagating structures of the form [11–13]

$$A(x,t) = a(x - vt)e^{i\phi(x-vt)}e^{-i\omega t} \ , \qquad (2)$$

where a and ϕ are real-valued functions of $z := x - vt$. Such structures play an important role in various dynamical regimes of the CGLE [10–13]. The substitution of Ansatz (2) into the CGLE leads to a set of three coupled ODEs for a, $b = da/dz$ and $\psi = d\phi/dz$ [14]. The MAWs correspond to limit-cycles of these ODEs, or equivalently, spatially periodic solutions of the CGLE. The MAWs occur in a two parameter family which we choose to parametrize by their spatial period P and their average phase gradient $\nu := 1/P \int_0^P dz\psi$. Some examples of MAWs are shown in Fig. 2b and Fig. 3. Only solutions for which $\nu = 0$ are considered here; the reason for this will be discussed in *(iii)*. To compute the MAWs and their bifurcations, we have used the software package AUTO94 [15] to solve the ODEs for fixed P and ν.

(ii) MAW range of existence - MAWs with $\nu \neq 0$ bifurcate from unstable plane waves in the CGLE. We focus on the $\nu = 0$ case, *i.e.*, on the homogeneous oscillation $A(x,t) = e^{ic_3 t}$. This solution becomes Benjamin-Feir (BF) unstable at $c_1 c_3 = 1$, beyond which all plane waves are unstable (Benjamin-Feir-Newell (BFN) criterion) [1]. In the ODEs, the fixed point $(a, b, \psi) = (1, 0, 0)$ that corresponds to the homogeneous solution undergoes a Hopf bifurcation (HB) upon increasing c_1 and c_3. For infinite P the Hopf bifurcation occurs for $c_1 c_3 = 1$, while for smaller P the Hopf bifurcation occurs for larger c_1 and c_3. The sequence of bifurcations for *fixed* $P = 50$ is illustrated in Fig. 2a. The square symbol denotes the Hopf bifurcation, and the resulting solutions have drifting velocity $v = 0$. Via a secondary drift pitchfork (DP) bifurcation [16] (diamond) the MAWs acquire $v \neq 0$. For the relevant parameters, *i.e.*, sufficiently small ν and large P, both bifurcations are supercritical [2]; the amplitude modulations grow away from these bifurcations. The MAWs

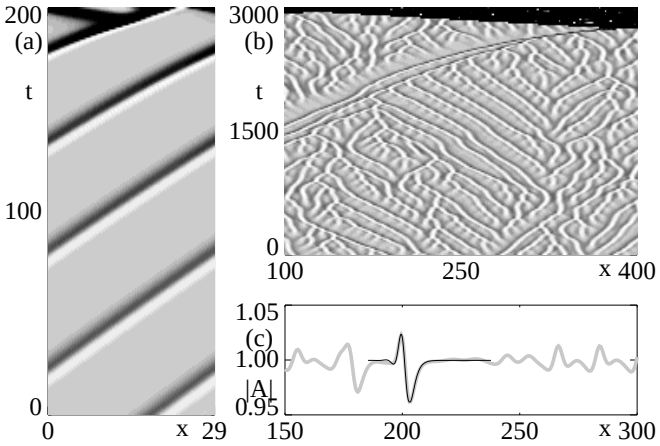

FIG. 3. (a) Grey-scale plot of $|A|$ (black: $|A| \to 0$) showing the nonlinear evolution of a near-MAW to defects when $L = 29 > P_{SN} = 26.8$ ($c_1 = 0.7, c_3 = 2$). (b) MAWs and defect generation in a transient phase chaotic state ($c_1 = 0.66, c_3 = 2.0$); a transient of $t \approx 10^4$ is not shown. (c) Comparison of a MAW (black) with a snapshot from a phase chaotic state (grey) ($c_1 = 0.66, c_3 = 2.0$).

undergo a saddle-node (SN) bifurcation (triangle) when c_1 or c_3 are sufficiently increased. The upper branch returns far back into the BF stable region of the CGLE; the recently discovered "homoclinic holes" [13] are MAWs of this upper branch in the limit $P \to \infty$. The spatial profiles of MAWs on the upper (II) and lower (I) branches and SN are shown in Fig. 2b.

The SN curves in the c_1–c_3 parameter plane have been computed for various spatial periods P. For given parameters c_1 and c_3, we define P_{SN} as the period for which a saddle-node bifurcation occurs. We find, roughly, that for larger P this SN occurs for smaller values of c_1, c_3 (see Fig. 1).

To summarize: a family of coherent, periodic MAW solutions of the CGLE has been obtained. The range of existence of these solutions is limited by a SN bifurcation for large c_1, c_3.

(iii) Beyond the Saddle Node - In Fig. 3 the relevance of the SN for defect generation is illustrated. In Fig. 3a we show the time evolution of a MAW-like initial condition in a periodic system of size $L > P_{SN}$. While for $L < P_{SN}$ we obtain coherent MAWs, for $L > P_{SN}$ incoherent dynamics occurs: the amplitude modulation and drifting velocity grow until defects are formed. Extensive tests show that defects are always generated for MAW-like initial conditions when $L > P_{SN}$. In Fig. 3b,c the relevance of this defect generating mechanism for chaotic states is illustrated in a *large* system of size $L = 512$ with coefficients close to the L_3 transition. The transient phase chaotic state (Fig. 3b) contains local structures which can come arbitrarily close to one-period MAWs. Fig. 3c shows a snapshot of a spatial profile of $|A|$ in a phase chaotic state; parts of this profile can be approximated

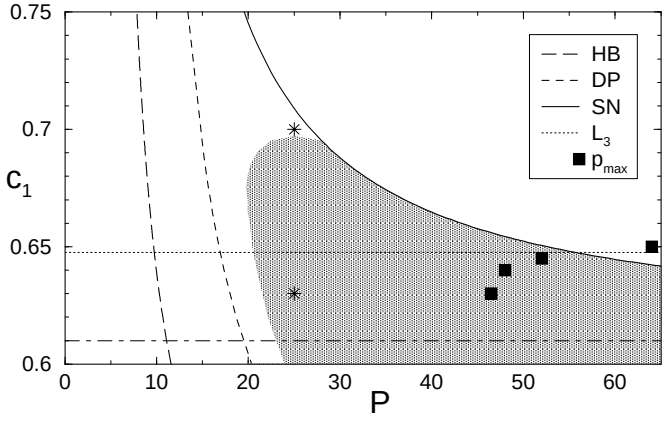

FIG. 4. Location of bifurcations and instabilities of MAWs as function of c_1 and P for $c_3 = 2.0$. Regions unstable to splitting modes are shaded. For large P, Hopf and drift pitchfork bifurcation approach the BFN line and the SN curve approaches $c_1 \approx 0.61$ (dot-dashed line). The two stars mark parameters corresponding to stability spectra shown in Fig. 5. Black squares show the numerically measured maximum peak to peak distance p_{max}; once these squares cross the SN curve, defects occur. This is consistent with the numerically found location of L_3 (dotted line).

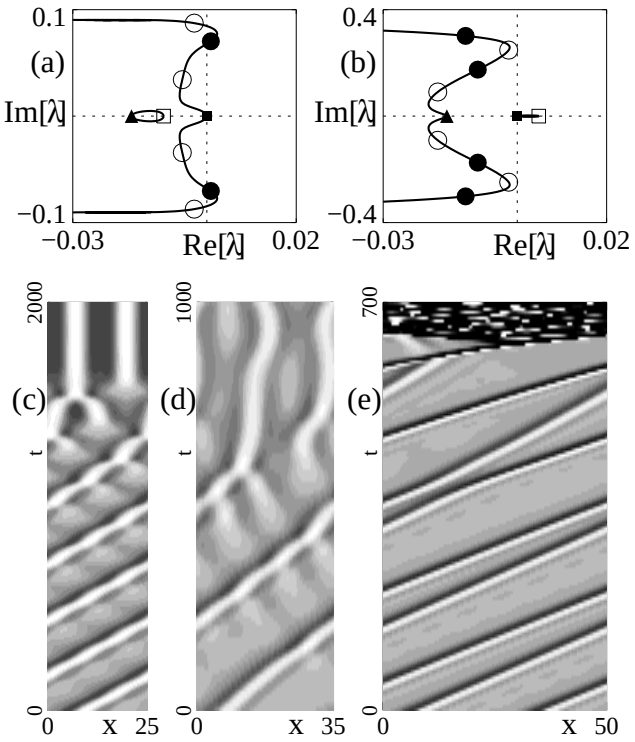

FIG. 5. (a-b) Two typical stability spectra for $c_3 = 2.0$, $\nu = 0$, $P = 25$ and (a) $c_1 = 0.63$ *resp.* (b) $c_1 = 0.70$. Filled symbols correspond to eigenvalues obtained for $L = P$, while open symbols denote additional eigenvalues for $L = 2P$ (symmetry modes: full square, splitting: circles, SN: triangle, interaction: open square); the curves show the spectrum for $L \to \infty$. (c-d) Illustration of the splitting instability that decreases p and prevents defects to occur ($c_1 = 0.63$). For small L (c) the splitting leads to a stationary pre-drift pitchfork MAW, but for larger L (d) disordered dynamics sets in. (e) Pulse interaction increases p beyond P_{SN} and leads to defects ($c_1 = 0.7$).

by a MAW with appropriate P. The phase gradient ν averaged between peaks of the amplitude is always close to zero; this is the reason why we focused on $\nu = 0$ MAWs. Defects appear when one of these MAWs acquires a period larger than P_{SN} (Fig. 3b). This illustrates the main result: the transition to defect chaos occurs when a phase chaotic state contains pulses with peak to peak distances larger than P_{SN}.

To test the generality of this picture, we have carried out extensive numerical simulations of Eq. (1) near the transition lines L_1 *resp.* L_3, adopting an integration algorithm developed in [11], in systems with sizes ranging from $L = 100$ to $L = 5000$ and integration times up to 5×10^6. The distribution of peak-to-peak distances p of the phase gradients has been determined. Even though the phase chaotic state is not everywhere MAW-like, we found that occurrences of large values of this "local" p were approximated well by MAW profiles. Defects occurred in systems with $L \geq 512$ if and only if $p > P_{SN}$. Since large p's are most "dangerous", the maximum value of p, p_{max}, is the relevant quantity here. An example of p_{max} as a function of c_1 near L_3 is shown in Fig. 4 (squares); as soon as p_{max} crosses the SN curve, defects occur.

One may worry whether p_{max} is a well-defined quantity, especially in the thermodynamic limit. For larger system sizes and integration times p_{max} increases, however the apparent transition where defects occur *shifts accordingly*. For example, we found in our simulations that for $c_3 = 2.0$, the critical value of c_1 approximates 0.65, while Ref. [7] finds, for shorter integration times, a critical value ≈ 0.68. The fact that p_{max} (slowly) increases for larger systems/longer times is in agreement with earlier assertions that there is no sharp transition to defect chaos [9]. We have not been able to establish an upper bound for the p's occurring in phase chaos; therefore we conjecture that the SN line for $P \to \infty$ provides a lower boundary for the transition from phase to defect chaos.

(iv) MAW stability - Of course, the laminar patches that occur in MAWs of large period are linearly unstable, and large P-MAWs have only a small probability to occur. To get some further insight in the behavior of MAWs, we have calculated the linear stability properties of the MAWs. We start with a system of size $L = P$ and periodic boundary conditions. Both MAW branches have neutral modes corresponding to translational and phase symmetries. The eigenvalue associated with the SN is positive for solutions on branch II and negative for

MAWs on branch I. Apart from these 3 purely real eigenvalues, the stability spectrum consists of pairs of complex conjugate eigenvalues.

In what follows the lower branch I is considered exclusively. For small enough P, all eigenvalues $\lambda_i < 0$, but when we increase P, MAWs become unstable to finite wavenumber perturbations. By using a Bloch Ansatz, we extended the stability analysis to systems with n identical pulses ($L = nP$). For $n > 1$, new instabilities may appear. The shape of these eigenmodes suggests that the instabilities lead to splitting of *resp.* interaction between adjacent MAWs; a nonlinear analysis confirms this. These instabilities are the relevant processes which locally decrease *resp.* increase p, thus inhibiting or enhancing the generation of defects. The splitting and interaction mechanism is very similar to the cell splitting and instabilities one encounters in the Kuramoto-Sivashinsky equation [4].

The results of the stability analysis are summarized in Fig. 4 and 5. It is important to stress here that there is no qualitative difference between the behavior of MAWs near the L_3 and the L_1 transition.

The eigenvalues with largest real part on the connected curve in Fig. 5a,b correspond to "splitting" modes; Fig. 5c,d displays the nonlinear evolution that occurs when this mode is unstable. Clearly, this instability tends to reduce the spatial periods p and prevents MAWs to cross the SN boundary. Above a critical value for c_1 (c_3) the splitting modes are stable for all P (Fig. 4). In this case the period of the MAWs can grow until $P > P_{SN}$ is reached and defects are created.

The eigenvalues labeled by open squares in Fig. 5a,b describe interaction between subsequent peaks that occur for $n > 1$ [17]. These interaction modes are mainly active for small P (typically $P < 20$). They cause instability of periodic MAWs and lead to local increase of the peak to peak distance p; Fig. 5e shows the nonlinear evolution in such a case.

Conclusion - We have presented a systematic study of modulated amplitude waves (MAWs) in the complex Ginzburg-Landau equation (CGLE). These periodic coherent structures originate in supercritical bifurcations due to the BF instability of the CGLE. MAW existence is bounded by saddle-node bifurcations towards large c_1, c_3. Approaching the transition from phase to defect chaos, near-MAWs with large P occur in phase chaos. Defects are generated if the period of these MAWs becomes larger than P_{SN}. This scenario is valid for both the L_1 and L_3 transition. Indications have been given in favor of the existence of the phase turbulent regime even in the thermodynamic limit. Altogether, our study leaves little space for doubt that the transition from phase chaos to defect chaos in the CGLE is governed by coherent structures and their bifurcations.

It is a pleasure to acknowledge discussions with H. Chaté and L. Kramer. AT and MB are grateful to ISI Torino for providing a pleasant working environment during the Workshop on "Complexity and Chaos" in October 1999. MGZ is supported from a post-doctoral grant of the MEC (Spain). MvH acknowledges financial support from the EU under contract ERBFMBICT 972554.

---

* Present address: Physics Department, FCEN-University of Buenos Aires, Pab. I Ciudad Universitaria, (1428) Buenos Aires, Argentina

[1] M. C. Cross and P. C. Hohenberg, Rev. Mod. Phys. **65**, 851 (1993).

[2] B. Janiaud, A. Pumir, D. Bensimon, V. Croquette, H. Richter and L. Kramer, Physica D **55**, 269 (1992).

[3] N. Mukolobwiez, A. Chiffaudel, and F. Daviaud, Phys. Rev. Lett. **80**, 4661 (1998).

[4] T. Bohr, M. H. Jensen, G. Paladin and A. Vulpiani, *Dynamical systems approach to turbulence* (Cambridge Univ. Press) (1998).

[5] B. I. Shraiman, A. Pumir, W. van Saarloos, P. C. Hohenberg, H. Chaté and M. Holen, Physica D **57**, 241 (1992).

[6] M. Bazhenov, M. I. Rabinovich and A. L. Fabrikant, Phys. Lett. A **163**, 87 (1994).

[7] H. Chaté, Nonlinearity **7**, 185 (1994); p. 33 in P. E. Cladis and Palffy-Muhoray (Eds.),"Spatio-Temporal Pattern Formation in Nonequilibrium Complex Systems" (Addison Wesley, Reading, 1995).

[8] H. Sakaguchi, Prog. Theor. Phys. **84**, 792 (1990).

[9] D. A. Egolf and H. S. Greenside, Phys. Rev. Lett. **74** 1751 (1995).

[10] R. Montagne, E. Hernández-García, and M. San Miguel, Phys. Rev. Lett. **77**, 267 (1996); R. Montagne, E. Hernández-García, A. Amengual and M. San Miguel, Phys. Rev. E **56**, 151 (1997).

[11] A. Torcini, Phys. Rev. Lett. **77**, 1047 (1996); A. Torcini, H. Frauenkron, and P. Grassberger, Phys. Rev E **55**, 5073 (1997).

[12] W. van Saarloos and P. C. Hohenberg, Physica D **56**, 303 (1992); **69**, 209 (1993) [Errata].

[13] M. van Hecke, Phys. Rev. Lett. **80**, 1896 (1998).

[14] The three ODE system reads: $a_z = b$;
$b_z = \psi^2 a - \gamma^{-1}[(1 + c_1\omega)a + v(b + c_1\psi a) + (c_1 c_3 - 1)a^3]$;
$\psi_z = -2b\psi/a + \gamma^{-1}[c_1 - \omega + v(c_1 b/a - \psi) - (c_1 + c_3)a^2]$.
Abbreviations used are $\gamma = 1 + c_1^2$, $a_z = da/dz, b_z = db/dz$ and $\psi_z = d\psi/dz$.

[15] E. J. Doedel, X. J. Wang and T. F. Fairgrieve, *AUTO 94: Software for continuation and bifurcation in ordinary differential equations*, Applied Mathematics Report, California Institute of Technology (1994).

[16] M. Kness, L. S. Tuckerman, and D. Barkley, Phys. Rev. A **46**, 5054 (1992).

[17] M. Or-Guil, I. G. Kevrekidis and M. Bär, Physica D **135**, 154 (2000).